

# Measurement and real-time cancellation of vibration-induced phase noise in a cavity-stabilized laser

Michael J. Thorpe,\* David R. Leibrandt, Tara M. Fortier, and  
Till Rosenband

National Institute of Standards and Technology, 325 Broadway St., Boulder, CO 80305, USA

[\\*mthorpe@nist.boulder.gov](mailto:mthorpe@nist.boulder.gov)

**Abstract:** We demonstrate a method to measure and actively reduce the coupling of vibrations to the phase noise of a cavity-stabilized laser. This method uses the vibration noise of the laboratory environment rather than active drive to perturb the optical cavity. The laser phase noise is measured via a beat note with a second unperturbed ultra-stable laser while the vibrations are measured by accelerometers positioned around the cavity. A Wiener filter algorithm extracts the frequency and direction dependence of the cavity response function. Once the cavity response function is known, real-time noise cancellation can be implemented by use of the accelerometer measurements to predict and then cancel the laser phase fluctuations. We present real-time noise cancellation that results in a 25 dB reduction of the laser phase noise power spectral density.

© 2010 Optical Society of America

**OCIS codes:** (140.3425) Laser stabilization; (140.4780) Optical resonators; (120.7280) Vibration analysis.

---

## References and links

1. B. C. Young, F. C. Cruz, W. M. Itano, and J. C. Bergquist, "Visible Lasers with Subhertz Linewidths," *Phys. Rev. Lett.* **82**, 3799–3802 (1999).
2. R. W. P. Drever, J. L. Hall, F. V. Kowalski, J. Hough, G. M. Ford, A. J. Munley, and H. Ward, "Laser phase and frequency stabilization using an optical resonator," *Appl. Phys. B* **31**, 97–105 (1983).
3. K. Numata, A. Kemery, and J. Camp, "Thermal-Noise Limit in the Frequency Stabilization of Lasers with Rigid Cavities," *Phys. Rev. Lett.* **93**, 250602 (2004).
4. M. Notcutt, L. S. Ma, J. Ye, and J. L. Hall, "Simple and compact 1-Hz laser system via an improved mounting configuration of a reference cavity," *Opt. Lett.* **30**, 1815–1817 (2005).
5. C. W. Chou, D. B. Hume, J. C. J. Koelemeij, D. J. Wineland, and T. Rosenband, "Frequency Comparison of Two High-Accuracy  $\text{Al}^+$  Optical Clocks," *Phys. Rev. Lett.* **104**, 070802 (2010).
6. B. Willke, K. Danzmann, M. Frede, P. King, D. Kracht, P. Kwee, O. Puncken, R. L. Savage, B. Schulz, F. Seifert, C. Veltkamp, S. Wagner, P. Weßels and L. Winkelmann, "Stabilized lasers for advanced gravitational wave detectors," *Class. Quantum Grav.* **25**, 114040 (2008).
7. T. Rosenband, D. B. Hume, P. O. Schmidt, C. W. Chou, A. Brusch, L. Lorini, W. H. Oskay, R. E. Drullinger, T. M. Fortier, J. E. Stalnaker, S. A. Diddams, W. C. Swann, N. R. Newbury, W. M. Itano, D. J. Wineland, and J. C. Bergquist, "Frequency Ratio of  $\text{Al}^+$  and  $\text{Hg}^+$  Single-Ion Optical Clocks; Metrology at the 17th Decimal Place," *Science* **28**, 1808–1812 (2008).
8. T. Nazarova, F. Riehle, and U. Sterr, "Vibration-insensitive reference cavity for an ultra-narrow-linewidth laser" *Appl. Phys. B* **83**, 531–536 (2006).
9. J. Millo, S. Dawkins, R. Chicreanu, D. V. Magalhaes, C. Mandache, D. Holleville, M. Lours, S. Bize, P. Lemonde, and G. Santarelli, "Ultra-stable optical cavities: Design and experiments at LNE-SYRTE," *Proc. IEEE Freq. Control Symp. (IEEE, 2008)*, pp. 110–114.

10. S. A. Webster, M. Oxborrow, S. Pugla, J. Millo, and P. Gill, "Thermal-noise-optical cavity," *Phys. Rev. A* **77**, 033847 (2008).
11. A. Hati, C. W. Nelson, D. A. Howe, N. Ashby, J. Taylor, K. M. Hudek, C. Hay, D. Seidel, and D. Eliyahu, "Vibration sensitivity of microwave components," *Proc. 2007 Joint Mtg. IEEE Int. Freq. Control Symp. and EFTF Conf. (IEEE, 2007)*, pp. 541–546.
12. A. Hati, C. W. Nelson, J. Taylor, N. Ashby, and D. A. Howe, "Cancellation of Vibration-Induced Phase Noise in Optical Fibers," *IEEE Phot. Technol. Lett.* **20**, 1842–1844 (2008).
13. N. Wiener, "Extrapolation, Interpolation, and Smoothing of Stationary Time Series," (The MIT Press, 1949).
14. J. C. Bergquist, W. M. Itano, and D. J. Wineland, "Laser Stabilization to a Single Ion," in *Frontiers in Laser Spectroscopy, proc. International School of Physics "Enrico Fermi"*, T. W. Hänsch and M. Inguscio eds. (North-Holland, Amsterdam, 2004), pp. 359–376.
15. L. S. Ma, P. Junger, J. Ye, and J. L. Hall, "Delivering the same optical frequency at two places: accurate cancellation of phase noise introduced by an optical fiber or other time-varying path," *Opt. Lett.* **19**, 1777–1779 (1994).
16. T. M. Fortier, A. Bartels, and S. A. Diddams, "Octave-spanning Ti:sapphire laser with a repetition rate >1 GHz for optical frequency measurements and comparisons," *Opt. Lett.* **31**, 1011–1013 (2006).
17. Z. W. Barber, C. W. Hoyt, C. W. Oates, L. Hollberg, A. V. Taichenachev, and V. I. Yudin, "Direct excitation of the forbidden clock transition in neutral  $^{174}\text{Yb}$  atoms confined to an optical lattice," *Phys. Rev. Lett.* **96**, 083002 (2006).
18. S. Haykin, "The LMS filter algorithm," in *Least-Mean-Square Adaptive Filters*, S. Haykin and B. Widrow eds. (Wiley, 2003), pp. xi-xiii.
19. J. Volder, "The CORDIC Trigonometric Computing Technique," *IRE Trans. Electronic Computing* **EC-8**, 330–334 (1959).
20. D. L. Jones, "Discrete-Time, Causal Wiener Filter," <http://cnx.org/content/m11825/latest/>.

## 1. Introduction

Lasers locked to well isolated Fabry-Perot cavities provide the highest short-term fractional-frequency stability [1]. For high-finesse cavities, the large signal-to-noise ratio (SNR) of the Pound-Drever-Hall (PDH) stabilization technique [2] allows laser frequencies to track the cavity resonance with negligible added noise. In this situation the laser's frequency stability is determined primarily by the length stability of the cavity. This length stability is limited fundamentally by intrinsic thermomechanical noise [1,3,4], but the thermomechanical noise can easily be exceeded by vibration-induced length changes. Such frequency-stable lasers play a crucial role in a wide range of scientific investigations including: optical atomic clocks [5], gravitational wave detectors [6], and searches for the time variation of fundamental constants [7], but their use is currently confined to quiet laboratory settings.

Since the first demonstration of thermal-noise-limited performance [1, 4], several designs have aimed at further reducing the sensitivity of the cavity reference frequency to external perturbations [4,9,10]. In these designs symmetries are exploited to reduce the sensitivity of the spacer length to seismic vibrations. However, residual asymmetries inevitably remain due to mechanical imperfections, limiting the sensitivity of the most vibration-insensitive cavities to about  $\delta L/L = 10^{-10}/g$  [8–10]. While this acceleration sensitivity matches the best radio-frequency crystal oscillators, it is likely too high for use in non-laboratory environments, and for field applications further reductions in sensitivity are desirable [11, 12].

In this work we discuss the application of Wiener filters [13] to measure the vibration sensitivity of a laser stabilization cavity, and to reduce this sensitivity with real-time corrections. This technique yields information about the cavity's vibration response function, which can be used to improve the mechanical design and minimize the residual vibration sensitivity. Here the natural vibrations of the laboratory floor act as the stimulus that allows the system's response function to be extracted. This simplifies the measurement, as no additional vibration drive is needed, but the low level of ambient vibrations limits the available measurement signal-to-noise ratio. Finally, the cavity response function is used to calculate real-time corrections to the laser frequency from measured accelerations and demonstrate a vibration-sensitivity reduction

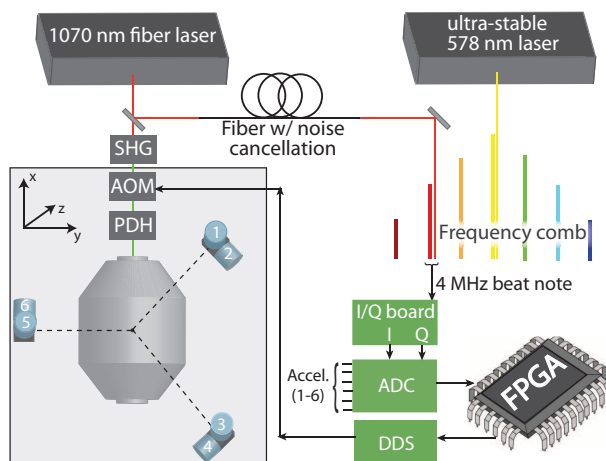


Fig. 1. The setup used to measure the cavity response functions and perform real-time noise cancellation. Six accelerometers (labeled 1-6) are positioned on the table such that (1,3,5) measure accelerations in the vertical ( $z$ ) direction while (2,4,6) measure accelerations in the horizontal ( $x,y$ ) plane. This combination of signals allows the measurement of all six motional degrees of freedom. The test light is transmitted to the frequency comb through a noise-cancelled optical fiber [14, 15], and the heterodyne beat note (mixed to approximately 4 MHz) measured at the frequency comb returns through a coaxial cable.

of 25 dB. The technique may yield higher sensitivity-reduction factors in an environment with stronger ambient vibrations.

## 2. Measurement setup

A schematic of the measurement setup is shown in Fig. 1. The laser for this experiment is a 1070 nm fiber laser that typically serves as the clock laser for probing the  $^1S_0$  to  $^3P_0$  transition in  $^{27}\text{Al}^+$  [5] (subsequently referred to as the test laser). The test cavity is built from a horizontally mounted, low-expansion glass spacer with a free spectral range of 625 MHz and a mirror reflectivity of  $R = 0.99999$  at 535 nm (corresponding to a finesse of 314,000) [1]. A PDH servo locks the second harmonic of the test laser to the optical cavity. When real-time noise cancellation is enabled, the cavity is ‘corrected’ for vibration-induced phase excursions by an acousto-optic modulator (AOM) that is driven by a rapidly-tunable digital synthesizer. The cavity, AOM and PDH optics rest on a steel plate (250 kg) that can be suspended from the ceiling with rubber bands [1] for passive vibration isolation. However, for many of the measurements presented here, the plate rests on the laboratory floor, so vibration noise couples directly to the optical cavity.

The phase of the test laser that tracks the stabilization cavity is measured via a heterodyne beat note with one frequency component of a self-referenced optical frequency comb [16] that is separately stabilized by locking it to an ultra-stable 578 nm laser [17]. The stabilized frequency comb serves as a low-noise reference with which the vibration-induced phase excursions of the test cavity can be measured through the phase excursions of the heterodyne beat note. This beat note is first mixed to near 4 MHz, and further mixed to near 0 Hz with a commercial demodulator circuit that yields separate in-phase and quadrature (I and Q) components of the signal. The I and Q components are sampled by a 14-bit analog-to-digital converter and further converted to phase samples with trigonometric functions. This system allows for a direct continuous measurement of the test laser’s phase. To determine the cavity response functions,

10 s to 100 s of acceleration and laser-phase measurements are recorded continuously on a PC with a sample rate of 1 kHz to 100 kHz. The recorded data is high-pass filtered in software with a 1 Hz corner to remove the DC component and then the optimal Wiener filter is extracted from the data.

When the system operates in real-time noise cancellation mode, the acceleration and phase measurements are input to a field-programmable gate array (FPGA). The FPGA uses a set of stored filter coefficients to predict the laser-phase excursions. After each phase prediction is calculated, the FPGA sends a phase tuning command to a direct digital synthesizer (DDS) to update the phase correction for the optical cavity via the AOM. The Wiener filter coefficients can be uploaded to the FPGA if they are available from previously processed data. Another approach, used for the real-time cancellation presented here, is to estimate the Wiener filter coefficients in real-time on the FPGA via a Least Mean Squares (LMS) algorithm [18]. With six accelerometer channels and 500 filter coefficients per channel, the update period for the system is about 1.4 ms. During this interval the following steps occur: eight analog-to-digital conversions (6 accelerometers plus I and Q signal components), conversion of I and Q samples to an absolute phase [19], Wiener filter coefficient update, phase prediction update, and finally the DDS phase update.

### 3. The Wiener filter and cavity response functions

The Wiener filter algorithm uses time domain correlation functions between the inputs and outputs of a linear time-invariant system to determine the predictable part of the system response in the presence of noise. For high SNR input data the algorithm calculates a set of time-domain filters that correspond to the finite impulse response of the system. We extend the discussion by Jones [20] to six accelerometer inputs. The discrete-time system model is

$$\hat{\phi}[n] = \sum_{m=1}^6 \sum_{k=0}^{N-1} h_{m,k} a_m[n-k]. \quad (1)$$

Here,  $\hat{\phi}$  is the model's predicted laser phase,  $n$  is the discrete-time variable,  $h_{m,k}$  is the  $k^{\text{th}}$  filter coefficient for the  $m^{\text{th}}$  input channel,  $a_m[n-k]$  is the signal from the  $m^{\text{th}}$  accelerometer at time delay  $k$ , and  $N$  is the total number of filter coefficients used for each input channel. The accelerometer signals  $a_m$  may be considered as the sum of true accelerations  $a'_m$  and accelerometer noise  $\varepsilon_m$ . The discrete-time  $n$  and continuous-time  $t$  are related by the sample rate  $f$ :  $t = n/f$ . The Wiener filter consists of the coefficients  $h_{m,k}$  that minimize the difference between the predicted phase  $\hat{\phi}$  and the measured phase  $\phi$  in a least-squares sense. This quantity,

$$e^2 = \sum_{n=-\infty}^{\infty} (\phi[n] - \hat{\phi}[n])^2, \quad (2)$$

is minimized by solving for the values of  $h_{m,k}$  that make  $e^2$  stationary, i.e.,  $\frac{\partial e^2}{\partial h_{m,k}} = 0$  for all values of  $m$  and  $k$ . This condition may be written as

$$\sum_{n=-\infty}^{\infty} \phi[n] a_i[n-j] = \sum_{n=-\infty}^{\infty} \sum_{m=1}^6 \sum_{k=0}^{N-1} h_{m,k} a_m[n-k] a_j[n-i], \quad (3)$$

and further rewritten in terms of correlation functions as

$$R_{\phi,a_i}[j] = \sum_{m=1}^6 \sum_{k=0}^{N-1} h_{m,k} R_{a_i,a_m}[j-k], \quad (4)$$

where  $R_{x,y}[j] = \sum_{n=-\infty}^{\infty} x[n]y[n-j]$ . The resulting set of  $6N$  equations can be solved for the  $6N$  filter coefficients  $h_{m,k}$ . Typically only one solution exists, which indicates that the calculated stationary point of  $e^2$  is indeed a minimum. These coefficients represent the optimal filter for predicting the effect of measured accelerations on the laser phase. In the limit of high SNR,  $h_{m,k}$  is the system's finite impulse response, i.e., the phase response to an impulse on accelerometer  $m$ .

For spectral regions where the acceleration measurements have a high SNR, the coefficients  $h_{m,k}$  can be used to determine the transfer function in the frequency domain. A discrete Laplace Transform, commonly referred to as the Z-Transform, converts the filter coefficients into transfer functions  $H_m(\omega)$  such that

$$\phi(\omega) = \sum_{m=1}^6 H_m(\omega)a_m(\omega). \quad (5)$$

While noise on the phase measurement has the effect of increasing the uncertainty of the transfer functions such that more averages are required to achieve a desired uncertainty in  $H_m(\omega)$ , accelerometer noise acts to change the values of  $H_m(\omega)$ , because terms of type  $R_{\varepsilon_i, \varepsilon_m}$  enter significantly on the right-hand-side of Eq. (4). The functions  $H_m(\omega)$  can be interpreted as transfer functions only when the accelerometer SNR is large. When the accelerometer SNR is

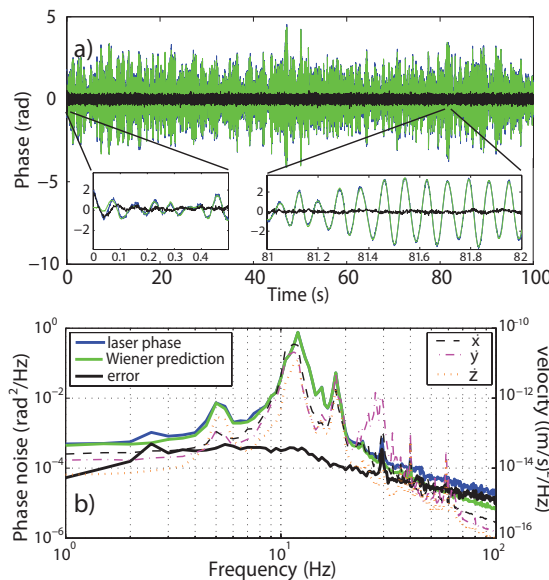


Fig. 2. (a) The time domain performance of the Wiener filter algorithm. The measured laser phase (blue), predicted phase (green) and residual error (black) show that the Wiener filter reduces the RMS phase fluctuations by more than an order of magnitude. The inset on the lower left shows the first 0.5 seconds of the time trace. Here, the error is initially large due to the lack of accelerometer information for times  $t < 0$  s. By  $t = 0.2$  s there is a sufficient history of accelerometer measurements to substantially reduce the phase error. The inset on the lower right shows the Wiener filter suppressing the RMS phase fluctuations of the laser by more than a factor of 10. (b) The phase noise power spectral density (PSD) of the measured phase, predicted phase and residual phase error showing more than 30 dB of noise cancellation at 12 Hz. The dashed traces show the velocity PSD measured by the accelerometers.

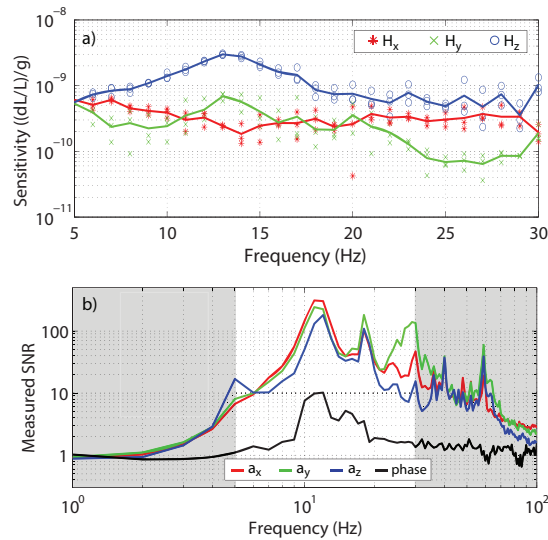


Fig. 3. (a) The fractional sensitivity of the cavity reference frequency to accelerations for the three translational (x,y,z) degrees of freedom in the 5-30 Hz spectral region. Three independent measurements were performed for each direction (markers) and the solid lines show the average values. (b) The measured SNR of the phase and acceleration measurements show that outside of the 5-30 Hz region, there is insufficient SNR to calculate the cavity acceleration sensitivity.

small, detailed knowledge of the noise characteristics is required to extract the transfer function.

To perform the Wiener filter analysis on the test laser, the cavity table was allowed to rest on the laboratory floor, where ambient seismic vibrations cause significant phase noise. A sample rate of 1 kHz and a nominal measurement time of 100 s were used to record the laser phase and accelerometer signals. The recorded data were then post-processed through the Wiener filter algorithm to determine the filter coefficients and the associated phase predictions. Figure 2(a) illustrates the time-domain performance of the Wiener filter with 600 filter coefficients for each accelerometer channel. The error trace shows that the residual phase noise after Wiener filtering is reduced by more than 30 dB at the peak noise frequency of 12 Hz.

Figure 3(a) shows the transfer functions for the translational degrees of freedom that resulted from an average of three independent sets of accelerometer and phase measurements. The transfer functions show that there is a low-Q resonance for vibrations in the z-direction (vertical) at 12 Hz. This resonance, together with the vibration noise peak near 12 Hz [Fig. 2(b)], accounts for the oscillatory behavior seen in the insets of Fig. 2(a). Analysis of the rotational degrees of freedom was unable to yield transfer functions, due to poor SNR. However, the large measured product of angular acceleration and cavity length suggests that the cavity is at least an order of magnitude less sensitive to angular accelerations than linear accelerations. Finally, Fig. 3(b) shows the measured SNR for both the phase and acceleration measurements. For the laser phase, the measured SNR is the ratio of the phase noise spectrum when vibration noise is coupled to the cavity versus when the cavity is isolated from vibration. For the accelerometer measurements, it is the ratio of the measured acceleration spectrum and the accelerometer noise floor. In spectral regions where these curves are close to 1, the transfer function calculation in Eq. (4) would require detailed knowledge of the accelerometer noise characteristics. We have not attempted to calculate the transfer function outside of the high SNR region of 5 Hz-30 Hz



shown in Fig. 3(b).

#### 4. The Least Mean Squares filter and real-time noise cancellation

To maintain high phase stability of the laser in noisy environments, the acceleration measurements are input into the embedded processor of an FPGA, which uses the filter coefficients to predict and then correct the laser phase in real-time. The recursive least mean squares (LMS) algorithm “learns” the values of the Wiener filter coefficients with much lower computational cost than the exact solution of Eq. (4) requires [18]. The LMS algorithm for six acceleration inputs and one phase output has much the same form as the Wiener filter algorithm. To derive the update equation for this filter, one follows the same procedure as for the Wiener filter shown in Eqs. (1) and (2). From this point the LMS algorithm minimizes the squared error between the model and the measured signal by relaxing the requirement that the minimization take place over all times. Accordingly, the minimization equation takes the form

$$\frac{\partial e[n]^2}{\partial h_{i,j}} = -2e[n]a_i(n-j) = 0, \quad (6)$$

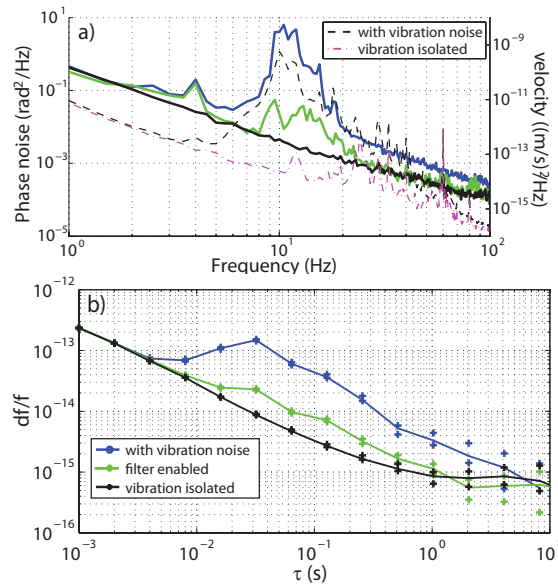


Fig. 4. (a) The laser phase PSD for three operating conditions: (1) the cavity table resting on the floor with the filter turned off (blue), (2) the cavity table resting on the floor with the filter turned on (green), and (3) the cavity table suspended by vibration isolating rubber bands (black). A real-time noise cancellation of 25 dB is achieved at 12 Hz compared to the free running case, but still several dB more than the vibration isolated case. The direction-averaged velocity PSD shows the effect of the rubber band suspension system in isolating the cavity from laboratory vibration noise. (b) The Allan deviation for the test laser in the three cases shown in (a). Without the LMS filter, the laser frequency instability increases by more than an order of magnitude at  $\tau = 0.1$  s and by a factor of 4 at  $\tau = 1$  s compared to the vibration isolated case (black). When the LMS filter is on, the test laser instability is within a factor of 2 compared to the vibration-isolated case for all time-scales. The points above and below each Allan deviation curve show the 90% confidence interval for the measurement.

where  $e[n] = \phi[n] - \hat{\phi}[n]$ . From Eq. (6), an update equation for the filter coefficients is constructed:

$$h_{i,j}^{n+1} = h_{i,j}^n - \mu \frac{\partial e[n]^2}{\partial h_{i,j}} = h_{i,j}^n + 2\mu e[n] a_i(n-j). \quad (7)$$

The coefficient  $\mu$ , referred to as the step size, determines the convergence rate and stability of the LMS algorithm. This algorithm performs a gradient search for the set of coefficients  $h_{i,j}$  that minimize the phase prediction error. At each time step the filter coefficients are updated via Eq. (7), and the current filter coefficients are used to calculate the next phase prediction  $\hat{\phi}$ . This prediction is compared to the measured phase  $\phi$  to determine  $e[n]$  for the next filter coefficient update. With the appropriate choice of  $\mu$ , the set of  $h_{i,j}$  quickly converges ( $\sim 10$  s) to the values obtained using the Wiener filter.

To perform real-time noise cancellation the filter updating is turned off ( $\mu = 0$ ), and the now static set of filter coefficients is used in conjunction with the accelerometer measurements to predict the laser phase excursions. The laser phase is corrected by subtracting the predicted phase excursion via the AOM in Fig. 1. Figure 4 shows the performance of real-time noise cancellation. Unlike the case of post-processed filtering, the real-time filtering shows some residual phase noise in the 8 Hz-20 Hz spectral region. The residual noise can be attributed to a combination of excess accelerometer noise that was present in the real-time measurements and the fact that the FPGA update rate had substantial timing jitter. Nevertheless, this initial implementation of real-time active vibration cancellation reduces the vibration sensitivity by 25 dB for the dominant ambient vibrations.

In future investigations it will be useful to carefully filter accelerometer signals and control the timing jitter of the FPGA output signals improve the real-time noise cancellation. Also, a study of the time-invariance of the cavity response will be required to determine how often the filter coefficients should be updated to maintain optimal noise cancellation.

## 5. Conclusion

We have measured the acceleration sensitivity of an optical cavity frequency reference with a Wiener filter algorithm that requires only ambient noise as the driving source. Furthermore, we have shown that the accelerometer measurements can be used for real-time cancellation of vibration-induced noise by up to 25 dB. Together with more robust and environment-insensitive cavity designs, the measurement and cancellation techniques presented here may allow cavity stabilized lasers to act as ultra-stable frequency references for non-laboratory applications.

## Acknowledgments

We thank Jim Bergquist, Dave Howe and Scott Diddams for useful discussions and Andrew Ludlow, Nathan Lemke and Yanyi Jiang for the use of their stabilized 578 nm laser. M. J. Thorpe and D. R. Leibrandt acknowledge support from the National Research Council. This work is not subject to U.S. copyright.